Difficulty of the evaluation of the barrier height of an open-shell transition state between closed shell minima: The case of small C-4n rings

Grégoire David, Gregoire David, Nadia Ben Amor, Tao Zeng, Nicolas Suaud, Georges Trinquier, Jean-Paul Malrieu

Difficulty of the evaluation of the barrier height of an open-shell transition state between closed shell minima: the case of small C_{4n} rings

Grégoire David[1], Nadia Ben Amor[2,*], Tao Zeng[3], Nicolas Suaud[2], Georges Trinquier[2] and Jean-Paul Malrieu[2]

[1] Univ Rennes, CNRS, ISCR (Institut des Sciences Chimiques de Rennes) − UMR 6226, F-35000 Rennes, France

[2] Laboratoire de chimie et physique quantiques, IRSAMC-CNRS-UMR5626, Université Paul-Sabatier (Toulouse III), 31062 Toulouse Cedex 4, France

[3] Department of Chemistry, York University, Toronto, ON, M3J1P3, Canada

Abstract

C_{4n} cyclacenes exhibit strong bond alternation in their equilibrium geometry. In the two equivalent geometries the system keeps an essentially closed-shell character. The two energy minima are separated by a transition state suppressing the bond alternation, where the wave function is strongly diradical. The paper discusses the physical factors involved in this energy difference and possible evaluations of the barrier height. The simple comparison between the restricted DFT/B3LYP for the equilibrium with the broken symmetry DFT/B3LYP of the transition state underestimates or cancels the barrier in comparison with the most reliable CASPT2 or NEVPT2 results. The minimal (2 electrons in 2 Molecular Orbitals) Complete Active Space SCF overestimates the barrier, the subsequent second-order perturbation cancels it. Due to the collective character of the spin-polarization effect, it is necessary to perform a full π CASSCF + second-order perturbation to reach a reasonable value of the barrier, but this type of treatment cannot be applied to large molecules. DFT procedures treating on an equal foot the closed-shell and open-shell geometries have been explored, such as MRSF-TDDFT and a new spin-decontamination proposal, namely DFT-dressed CI, but the results still depend on the density functional. The M06-2X without or with spin-decontamination gives the best agreement with the accurate wave function results.

*Corresponding author: benamor@irsamc.ups-tlse.fr

I) Introduction

The present paper formulates a methodological challenge: what may be an appropriate quantum chemical computational technique for the evaluation of the isomerization barrier between two isomers of essentially closed shell (CS) character when the transition state (TS) is of open-shell character? We consider the C_{4n} cyclacenes as paradigmatic of this situation. Their ground state geometry exhibits a strong bond-length alternation of the CC bonds. There exist two degenerate isomers, obtained by interchanging short and long bonds. The chemical isomerization from one isomer to the other goes through a transition state geometry where all CC bonds have practically equal bond lengths. The simplest mono-electronic descriptions, starting from the Hückel Hamiltonian, predict that for the regular (non bond-alternating) geometry a degeneracy takes place between the two highest occupied molecular orbitals (MOs), which become singly occupied MOs (SOMOs). They transform as two components of an *E*-type irreducible representation and cannot interact. The system is then a pure diradical, since as will be discussed later, the wave function does not have any ionic component. The geometrical distortion introduces a strong bond alternation and breaks the symmetry, split the energies of the SOMOs, the lowest-energy one becoming doubly occupied. The phenomenon is usually described as a pseudo-Jahn-Teller distortion[1–4]

Then along the isomerization reaction path, an initially closed-shell wave function converts into a diradical function, before returning to a closed-shell character. The wave function for the essentially closed-shell minima may *a priori* be constructed from a closed-shell single determinantal approximation, even if correlation effects may be added later. Oppositely the zero-order description of the transition state is intrinsically bi-determinantal. Section II will discuss the methodological challenge raised by this qualitative difference between the minima and the transition state.

Single-determinant approaches may nevertheless be employed. Around the equilibrium geometries the optimization of the MOs will lead to a closed-shell single determinant, either in the Hartree-Fock self-consistent field (SCF) or in the Kohn-Sham Density Functional Theory (DFT) formalisms. For the transition-state geometry a spin-symmetry breaking takes place, defining different MOs for different spins, in the so-called Unrestricted or Broken Symmetry (BS) formulation[5–7] of the SCF or DFT methods. The wave function passes smoothly from the restricted to the BS solutions somewhere between the equilibrium and the

transition state, as occurs in stretching of the homopolar single bonds. However, the BS single determinants are not eigenfunctions of the S^2 operator, they are spin-contaminated. A spin-decontamination[8–16] seems a minimal pre-requisite for a DFT estimation of the barrier height. The description of open-shell low spin states is a well-known challenge in DFT and especially in the context of the evaluation of singlet-triplet gaps, leading to various DFT-based proposals to overcome the problem raised by the use of BS determinants.[17–21] The simplest spin-decontamination using a unique single S^2 mean-value presents severe defects as shown in refs [14,15]. The best procedure will consist in rigorous projection on symmetry-adapted spaces as suggested by Scuseria from wave function theory (WFT) solutions.[12,13] A simpler solution has been recently proposed by some of us.[16] Another way is to eliminate spin-contamination of spin-[17,20,18,19,21]flip (SF) time-dependent (TD)-DFT method by the use of mixed-reference reduced density matrix (MRSF-TDDFT).[22]

Moving back to wave-function based methods (WFT), one may consider that since the transition state requires to consider 2 electrons in 2 MOs (namely the two SOMOs), one should as well treat the two upper-energy electrons in the set of the Highest Occupied MO (HOMO) and Lowest Unoccupied MO (LUMO) and perform a Complete Active Space SCF[23] with 2 active electrons in 2 active MOs (CASSCF (2,2)), which in principle treats both geometries on an equal foot. From this simple description correlation effects might be estimated using standard multi-reference perturbation theories.

The numerical results reported in section III show the failure of these simple approaches:

1. Comparing the restricted DFT/B3LYP[24–27] energy for the closed-shell geometry with the BS-DFT/B3LYP energy of the transition state the barrier disappears or is extremely small, which is unlikely.
2. The CASSCF (2,2) barriers are very large, while the second-order perturbation puts the non-alternating geometry well below the alternating one.

This situation compels to improve the computational tools. We first try to assess a reasonable value of the barrier from intensively correlated WFT methods. A previous work[28] has shown that the spin-polarization effect, particularly important at the transition state, presents a cooperative character, and requires a full π CASSCF followed by a second-order perturbation treatment. This treatment may be consistently applied to both geometries and provides a

reliable evaluation of the barrier. Being costly, these computations have been performed on small C_{4n} rings only (n=3 or 4).

For large rings, a consistent DFT based treatment would definitely be welcome. Based on an analysis of the physical factors governing the singlet-to-triplet gap in diradicals, recent works have proposed a rigorous procedure exploiting BS-DFT computations and providing spin-contamination free energies[15,16]. We propose in section IV a consistent extension of this treatment for the geometries where the DFT solution is of closed-shell character. These results will be compared to those of MRSF-TDDFT and of the best WFT methods.

II) Physics of the problem and methodological challenges.

C_{2n} rings are alternant hydrocarbons (free from odd-membered rings) *i.e.* one may give one of two colors (red and blue) to each atom in such a way that each atom of a given color is linked to atoms of the other color. In these rings the numbers of red- and blue-colored atoms are equal. The Ovchinnikov's rule[29], which may be demonstrated from Heisenberg or from Hubbard[30,31] Hamiltonians, says that ground state is a singlet state. In the monoelectronic Hückel Hamiltonian or in any mean-field calculation a regular C_{4n} ring exhibits two degenerate singly-occupied Molecular Orbitals. These MOs belong to two irreducible symmetry representations. The wave function is invariant under the rotation of the two SOMOs, and according to the so-called "mirror theorem"[32] it is possible to define a set of SOMOs where one of them is localized on the blue atoms while the other is localized on the red ones. Let us call *a* and *b* these two SOMOs. The singlet wave function may be written as a linear combination of two degenerate determinants

$$\Psi_N^1 = \left|\Pi_k k\overline{k}.(a\overline{b} + b\overline{a})\right|/\sqrt{2}$$

where k runs on the closed-shell MOs. The subscript N indicates that the configuration is "neutral", each SOMO bearing only one electron, the superscript refers to the spin multiplicity. A triplet state belongs to the same space configuration, the m_s=0 component of which is

$$\Psi^3 = \left|\Pi_k k\overline{k}.(a\overline{b} - b\overline{a})\right|/\sqrt{2}.$$

In principle the minimization of the BS-DFT determinant

$$\Phi_{U,a'\overline{b}'} = \left|\Pi_k k' \overline{k''}.a'\overline{b}'\right|$$

incorporates two distinct effects. The mixing of the orthogonal SOMOs *a* and *b* in *a'* and *b'* introduces ionic components in the wave function (and therefore reduces $<S^2>$), while the spin-dependent relaxation of the core MOs *k'* and *k''* treats partially the spin-polarization effect, to the price of increasing $<S^2>$.(13) The popular Yamaguchi correction[8–11], supposed to offer a spin decontamination of the BS-DFT solution, treats both effects as the first one and is not reliable[11]. In the C_{4n} series the spin polarization is the only actor, for large values of n, $<S^2>$ reaches values close to 2, which would explode the correction.

Notice that for C_{4n} rings at the transition state there is no ionic component in the wave function, t_{ab}=0, and *a* and *b* do not relax in *a'* and *b'*. The BS-DFT evaluation of its energy simply incorporates a biased evaluation of the spin-polarization, as detailed in section V.

In the CS wave function relative to the equilibrium geometry

$$\phi_{CS} = \left|\Pi_k k\overline{k}.g\overline{g}\right|$$

the two upper-energy electrons occupy the same *gerade* HOMO. An *ungerade* virtual MO *u* (the LUMO) may be associated by the mirror theorem[32], and the *g/u* set of MOs span a set of localized MOs *a* and *b*, similar to the previously defined SOMOs. The CS determinant imposes a half-and-half ratio of the neutral (left) and ionic (right) Valence Bond components

$$\phi_{CS} = \left|\Pi_k k\overline{k}.\left(a\overline{b} + b\overline{a}\right) + \left(a\overline{a} + b\overline{b}\right)\right|/2,$$

while the second component is of higher energy. The left/right or neutral/ionic correlation is missing, while in the TS geometry the ionic component is zero and the ionic component de-mixing is correctly taken into account. Moreover, the CS description totally ignores the spin-correlation between the two upper-energy electrons and the core electrons. One understands that the physics incorporated in, respectively, the CS and BS treatments is not balanced, to the disadvantage of the CS geometry.

One may go beyond the single determinant evaluation in either the WFT or the DFT philosophies. In the WFT approach one should at least treat correctly the interaction of the 2 upper electrons in the HOMO/LUMO set, through a CASSCF (2,2) treatment. This treatment misses the correlation between these 2 electrons and the core, which is expected to stabilize

the TS, and the barrier should be too large. One may attempt a perturbative treatment of the correlation beyond CASSCF (2,2) according to the CAS second-order perturbation theory (CASPT2) method[33,34] or the N-electron valence state second-order perturbation theory (NEVPT2)[35,36] in its strongly contracted formulation. In CASPT2 it is recommended to introduce an empirical IPEA shift[34] to get a better balance between essentially closed-shell and essentially radical situations. Since the use of the IPEA shift is a matter of debate[37–46] calculations without and with standard IPEA (0.25 a.u.) have been performed on all systems. NEVPT2 is parameter-free and will be considered as the reference method in all the study.

A previous work[28] has shown that spin-polarization is a cooperative effect, which means that the spin-polarization of a given shell favors the spin-polarization of the other shells. This means that the treatment of spin polarization requires to introduce products of single excitations, *i.e.* multiple excitations. If spin polarization plays an important role in the barrier height, one should go to high excitation levels in the π system and perform at least full valence π CASSCF calculations. They miss the non-negligible spin-polarization of the σ core electrons, which has to be evaluated at least from a second-order perturbation.

The last section first reports the results of spin-contamination free method, MRSF-TDDFT. A recent work[16] has proposed a correct use of BS-DFT calculation, treating correctly the three main contributions, namely, direct exchange, kinetic exchange and spin-polarization. It may be applied to the TS geometry. An extension of this approach to the closed-shell geometry will be explored in the last section.

III) Numerical studies

The calculations have been performed using Gaussian[46] (DFT), Molcas[47–49] (CASSCF/CASPT2), GAMESS (MRSF-TDDFT)[50] or Orca[51] (DFT[52], CASSCF/NEVPT2) packages. The 6-311G** basis set has been used throughout this work. The impact of enlarging the basis set has been tested on the smaller compound.

A) Choice of systems and DFT/B3LYP geometry optimizations

We consider five C_{4n} rings, namely the cyclobutadiene, a centro-saturated phenalene $C_{13}H_7$, crown-shaped $C_{16}H_{16}$ and an internally saturated C_{16} ring, $C_{19}H_{13}$ (Figure 1). We have added another C_{12} ring, namely the carbo-cyclobutadiene, $C_{12}H_4$, the π conjugated system of which involves 12 π electrons. The DFT geometry optimizations have been performed using the B3LYP[24–27] functional in the (6-311G**) basis set. All the geometries are given in Table 1.

For the cyclobutadiene, the closed shell structure exhibits a strong contrast between short (1.332 Å) and very long (1.579 Å) bonds while a D_{4h} symmetry is kept for the BS structure with an intermediate value (1.440 Å) for the CC bond length . The carbo-cyclobutadiene, the less typical member of the series, exhibits two triple bonds and two cumulenic systems with four different CC bond length for the CS minimum (D_{2h}) and only two, keeping the D_{4h} symmetry, for the BS transition state. The closed-shell treatment always provides clear bond length alternation and marked deviations from planarity in $C_{13}H_{10}$ and $C_{19}H_{13}$. In these systems the double bonds keep an in-plane geometry while the single bonds are twisted. The CC double bond lengths are between 1.351 and 1.352 Å for the $C_{13}H_{10}$ and between 1.354 and 1.361 Å for the larger $C_{19}H_{14}$ system. The long lengths are typical of sp^2-sp^2 single bonds: 1.454/1.455 Å and 1.443/1.452 Å for $C_{13}H_{10}$ and $C_{19}H_{14}$ respectively.

The considered $C_{16}H_{16}$ system is not the most stable isomer but is a true minimum and the most regular one. For various structural studies of 16-annulenes, see for instance refs. [53–60]. This crown-shaped geometry presents a bond-length alternation (1.449/1.360 Å).

For all these five systems, the BS treatment converges on practically equal bond lengths with a very small deviation of the CC bond lengths from the ideal value 1.40 Å. Furthermore, despite the introduction of internal sp^3 carbons the conjugated rings are almost planar in $C_{13}H_7$ and $C_{19}H_{13}$. The Hessian presents a single negative root, the imaginary frequency being very low, and the associated change of geometry corresponds to the creation of bond-length alternation.

Of course, the DFT/B3LYP optimized geometries are not necessarily the exact ones, but they are sufficiently distinct to discuss the methodological problem of the energy difference between two closed-shell geometries and the diradical transition state (TS) and, even if the DFT/B3LYP geometries deviate slightly from the exact ones, their energy difference between these geometries should be close to the barrier height.

The HOMO/LUMO and SOMOs are pictured in figure 2. For the four first systems, the SOMOs are found similar to the bond-centered HOMO/LUMO but due to their degeneracy they may be transformed into atom-centered as directly obtained in the $C_{19}H_{14}$ compound.

B) Evaluations of barrier heights

For all systems, the energy difference between the closed and open-shell geometries are evaluated by means of DFT/B3LYP, with a closed-shell description for the CS geometry and a broken-symmetry one for the open-shell geometry. The zero-point energy (ZPE) is also evaluated (Table 2). Furthermore, the energy difference is also calculated by CASSCF + perturbation treatments, using a CAS(2,2) or a full π active space. The CAS(2,2) does not necessary provide meaningful SOMOs or HOMO/LUMO pairs as discussed for instance in the case of $C_{16}H_{16}$.

1) C_4H_4

The direct DFT/B3LYP calculations without any spin decontamination suggest a barrier of 2.2 kcal/mol. Using the same basis set, a minimal CAS(2,2) active space gives a larger barrier of 12.1 kcal/mol at the CASSCF level while the CASPT2, without IPEA, is reversed, with a value of -7.0 kcal/mol. When an IPEA shift of 0.25 a.u. is applied, the CASPT2 "barrier" remains slightly negative, -1.3 kcal/mol, while SC-NEVPT2 gives a small positive value of 0.7 kcal/mol. When all the π orbitals are included in the active space (Full π), the CASSCF(4,4) gives a barrier of 6.1 kcal/mol, to be compared with the value of 4.8 kcal/mol obtained by a previous MCSCF study with a smaller 6-31G* basis set.[4] In order to evaluate the influence of the basis sets on our results, a larger 6-311++G(3df,3pd) basis set was also used and the CASSCF barrier value is of 6.7 kcal/mol (+0.6 kcal/mol compared to the 6-311G** basis set). As expected, the effect on the B3LYP result is small (+0.2 kcal/mol). The NEVPT2 treatment enhances the barrier to 8.4 kcal/mol (*8.7 kcal/mol with the largest basis set*). The corresponding CASPT2 result without IPEA lowers this value to 3.3 kcal/mol (*3.1 kcal/mol*); but adding the IPEA shift of 0.25 a.u. the barrier returns to 6.4 kcal/mol (*6.7 kcal/mol*). The effect of enlarging the basis set is quite small for all these methods and the 6-311G** can be considered as sufficient to treat the larger systems. However, in view of these discrepancies we have tried to perform an enlarged CASSCF calculation, adding the valence MOs relative to the sigma CC MOs (bonding and antibonding). This enlarged CASSCF calculation enhances the barrier to 10.9 kcal/mol, the PT2

correction lowers it to 5.0 without IPEA, or to 7.1 with IPEA=0.25 a.u. These results can be compared to the 6.4 kcal/mol given by coupled - cluster method with full inclusion of the triple excitations (CCSDT) and 6.6 kcal/mol from MR - CCSD(T) .[61] These calculations were done with a smaller split-valence (3s2p1d/1s) basis set.

The dispersion of the results shows the difficulty to perform consistent calculations on the same system in two geometries where the ground state is physically very different. They nevertheless indicate the need to introduce the empirical IPEA shift in CASPT2 calculations to avoid an over-stabilization of the diradical TS, and confirm that the barrier is about 6.4 to 8.4 kcal/mol, much larger than the crude DFT/B3LYP value.

2) Carbo-cyclobutadiene $C_{12}H_4$

Despite the existence of non-conjugated π bonds in the σ plane of the molecule, the π electron system involves 12 electrons and behaves as an anti-aromatic ring. For B3LYP the BS minimum is 2.7 kcal/mol *below* the closed shell solution. Actually, one finds a BS solution even in the closed-shell preferred geometry, as illustrated in Figure 3, which follows the energies of both solutions along a linear synchronous transit (LST) between the two geometries. It is however unlikely that this molecule is a diradical. The collective character of the spin-polarization phenomenon has been demonstrated on this precise problem[28] and its partial incorporation in the BS treatment at the DFT level may induce a bias in favor of the D_{4h} geometry.

The CASSCF (2,2) treatment suggests a very high barrier (24.7 kcal/mol) while the CASPT2 without IPEA over-stabilizes the D_{4h} structure, down to -17.6 kcal/mol and -4.1 kcal/mol with the 0.25 a.u. IPEA value while NEVPT2 gives -20.6 kcal/mol. These numbers show the importance of correlation effects and the difficulty to treat them perturbatively. Going to the full valence π CASSCF (12,12) level the barrier is reduced to 6.1 kcal/mol. To confirm the role of the spin polarization, an additional calculation is done, namely a RASSCF starting from the CAS(2,2) adding 1 hole, 1 particle in the 10 other π MOs. Indeed, the barrier is reduced from 24.7 to 2.3 kcal/mol. A CASPT2 treatment on top of the CAS(12,12) destroys the barrier to -1.9 without IPEA, and reduces it to 2.6 kcal/mol with 0.25 a.u. IPEA. This last estimation seems to be confirmed by the result of the parameter-free NEVPT2 method, applied on top of the CASSCF(12,12) eigenfunctions, which finds a barrier of 2.3 kcal/mol.

Figure 4 reports the evolution between the bond-alternating geometry and the transition state for full π CASSCF, CASPT2 (without and with IPEA shift) and strongly or partially contracted NEVPT2 methods. One cannot rely neither on the CASSCF nor the CASPT2 results without IPEA. One can notice the remarkable agreement between the partially and strongly contracted NEVPT2 versions. The consistent results of the NEVPT2 and the CASPT2 with IPEA methods suggest that the bond length alternation at the minimum is less pronounced than the result obtained by DFT/B3LYP. It is not so surprising that such large correlation effects on the energy difference between two extreme geometries also impact the optimum bond-length alternation.[62]

3) Internally saturated phenalene, $C_{13}H_{10}$

In DFT/B3LYP, the BS solution is only 0.5 kcal/mol above the closed-shell one. The minimal CASSCF(2,2) treatment gives a huge barrier (25.2 kcal/mol), the state ordering being reversed at the NEVPT2 level to -10.9 kcal/mol. This discrepancy demonstrates that the physics taking place beyond the minimal CAS cannot be treated perturbatively. The natural next step consists in performing a CASSCF (12,12) of the π valence space. The CASSCF energy difference is 9.4 kcal/mol, and 4.4 kcal/mol at the NEVPT2 level. The CASPT2 values without IPEA suggests the unlikely existence of three degenerate minima as the BS energy is found identical to that of the CS one. The 0.25 a.u. IPEA shift restores the barrier with a reasonable agreement (5.1 kcal/mol) with the NEVPT2 result.

4) Crown-shaped $C_{16}H_{16}$

There is no bond alternation according to DFT/B3LYP, the closed shell minimum is found 0.9 kcal/mol above the BS one. In that case, the CASSCF(2,2) at the open-shell geometry leads to an essentially single-determinant closed-shell wave-function. The active orbitals are either localized on a unique π bond or delocalized, as expected, on the whole π system but, in the two cases, with occupation numbers close to 2 and 0. The values reported in Table 3 are then irrelevant and are given in parenthesis. This problem disappears when performing the full π CASSCF which predicts a large barrier (10.3 kcal/mol) while the CASPT2 without IPEA, as in the previous systems, over-stabilizes the non-alternating geometry. The CASPT2 with 0.25 a.u.

IPEA produces reasonable value of 4.4 kcal/mol. This value is practically identical to that obtained from NEVPT2 (4.6 Kcal/mol).

5) Graphanized $C_{19}H_{14}$ ring

The internally graphanized $C_{19}H_{14}$ nano-flake, which exhibits a peripheral conjugated C_{16} ring, has also been studied through an all π valence CASSCF calculation. The DFT/B3LYP calculations converge to two well-characterized minima. The two singly-occupied MOs are essentially localized on "red" and "blue" sites as in CASSCF (see Fig.2). The closed-shell solution is lower by 1.0 kcal/mol only. The convergence of the CASSCF(2,2) is difficult and predicts a huge barrier of 40.7 kcal/mol. The corresponding NEVPT2 reverses the result (-8.1 kcal/mol). The full valence π CASSCF(16,16) calculation still predicts a large barrier (12.0 kcal/mol), which is dramatically cancelled to -0.7 kcal/mol by the CASPT2 treatment without IPEA. The recommended IPEA value restores a barrier to 6.0 kcal/mol. The NEVPT2 result was not obtained.

6) Summary

These evaluations of the barriers are summarized in Tables 3 and 4. The most reliable estimates are those provided by the valence π CASSCF + NEVPT2 or CASPT2 with the large value of the empirical IPEA parameter (0.25 a.u.). Without the perturbative correction the barrier is too large. The minimal CASSCF (2,2) gives exceedingly large values and the second-order perturbation eliminates the barrier, with a deep diradical minimum. Comparing the DFT/B3LYP energies of the closed shell determinant for the minimum to that of the BS solution for the TS similarly destroys the barrier or propose a severely underestimate of its value. But the large CASSCF+ PT2 cannot be applied to large rings and an improvement of DFT approaches would be welcome.

IV) Search of reliable DFT-based barrier energies

As previously noticed, one cannot rely on methods which treat differently the equilibrium geometry from a closed-shell description and the transition-state geometry from an open-

shell approach, since the physics incorporated in these treatments are different. One needs a uniform treatment. We consider two proposals satisfying this requirement, namely the Mixed-Reference Spin-Flip Time-Dependent DFT and a new proposal, DFT-dressed CI. But of course one cannot forget the impact of the choice of the exchange-correlation potential, which will be discussed in the last part of this section.

A) Mixed-Reference Spin-Flip Time-Dependent Density Functional Theory

The details of MRSF-TDDFT are presented in Refs. [22,63–65]. Only a brief overview of this method is given here. MRSF-TDDFT was devised to solve the spin contamination problem of conventional the SF-TDDFT method. After a regular restricted open-shell Kohn-Sham DFT calculation with a setting of triplet spin multiplicity, a $|\Pi_k k\bar{k}.ab|$ type Kohn-Sham determinant is obtained as the reference triplet state with m_S = +1. M_S is the magnetic quantum number of the total spin. ab here represent the two generic SOMOs with α spin and can be replaced by gu. Then a mixed-reference reduced density matrix is constructed, equally averaging the density matrix of this reference state and that of its m_S = -1 analogue, $|\Pi_k k\bar{k}.\bar{a}\bar{b}|$. The Tamm-Dancoff approximation is then applied to such a mixed-reference reduced density matrix, resulting in decoupled linear-response equations of singlet and triplet states. There is hence no spin contamination in the resultant singlet and triplet (with m_S = 0) states obtained from one-electron excitations and de-excitations along with spin-flipping.

The $a \rightarrow \bar{a}$ and $b \rightarrow \bar{b}$ spin-flippings in the $|\Pi_k k\bar{k}.ab|$ reference and the spin-reversed counterparts in the $|\Pi_k k\bar{k}.\bar{a}\bar{b}|$ reference result in the singlet open-shell diradical configuration, and also the corresponding triplet configuration with m_S = 0. The spin-reversed counterparts will not be mentioned below but they are implicitly included. The $a \rightarrow \bar{b}$ and $b \rightarrow \bar{a}$ spin-flippings and electron transfers result in the $|\Pi_k k\bar{k}.a\bar{a}|$ and $|\Pi_k k\bar{k}.b\bar{b}|$ ionic configurations, which can interact with the singlet open-shell diradical configuration through the transfer integral t_{ab}. The spin-flipping and excitation of one electron from a doubly occupied orbital h to a virtual orbital p results in the $|\Pi_{k\neq h} k\bar{k}.\bar{p}ab\bar{h}|$ and $|\Pi_{k\neq h} k\bar{k}.p\bar{a}\bar{b}h|$ type configurations, where p and h stand for particle and hole orbitals. These configurations (labeled as Type IV in Ref. [22] and shown in the middle of Figure 13 of Ref. [66]), provide spin polarization in mixing with the singlet open-shell diradical configuration.

The collinear spin-flipping (SF) mechanism is used in MRSF-TDDFT. In the collinear SF mechanism, configurations obtained by different SF transitions are only coupled by exact exchange.[67] Therefore, MRSF-TDDFT shall be used along with a functional with a large fraction of exact exchange. We chose the BHHLYP[24] functional in this work in our MRSF-TDDFT calculations, following the developers of this method[22,63,64]. Overall, the advantages of MRSF-TDDFT include : (1) the method is parameter-free (other than the parameters in the functional); (2) the resultant states are free from spin contamination; (3) electronic structures at different geometries are treated on the same footing; (4) it is an inexpensive replacement of multireference WFT calculations; (5) it is straightforward to generalize the analytic gradient algorithm of SF-TDDFT to MRSF-TDDFT, and this has been accomplished[63]; (6) it is fairly accurate, as it exhibits a ~ 0.14 eV (3.2 kcal/mol) mean absolute error in evaluating adiabatic singlet-triplet (ST) gaps[64].

B) A DFT-dressed CI method

Let us recall first our recent proposal for a consistent spin-decontaminated evaluation of the energy of diradicals[16]. The method was proposed in the context of research of Singlet-Triplet energy gaps, and was based on the analysis of the physical factors governing this energy difference in WFT methods (see 51, 53). A transposition to DFT approaches was possible and led to a decomposition of several contributions,[68] from a few set of constrained DFT computations[15,16]. By the way a perfectly spin-contamination free method was proposed.[16] Let us summarize its content for the geometries where the lowest energy single determinant is of BS character.

As for the MRSF-TDDFT one starts from the definition of a closed-shell core and of SOMOs from the energy minimization of a restricted open-shell triplet determinant

$$\Phi_{ab}^{R} = \left|\Pi_k k\bar{k}.ab\right|,$$

of energy $E_{ab}^{R} = \left\langle \Phi_{ab}^{R} \middle| H \middle| \Phi_{ab}^{R} \right\rangle$. The two localized SOMOs *a* and *b* generate symmetry-adapted MOs *g* and *u,* or HOMO and LUMO, by a 45° rotation, $\Phi_{ab}^{R} = \left|\Pi_k k\bar{k}.gu\right|$.

Then one defines a restricted singlet configuration, which appears to be "neutral" with one electron only in the localized MOs *a* and *b*

$$\Psi^1_{ab} = \Psi^1_N = \left|\Pi_k k\bar{k}.(b\bar{a} + a\bar{b})\right| / \sqrt{2} = \left|\Pi_k k\bar{k}.(g\bar{g} - u\bar{u})\right| / \sqrt{2}\,.$$

The energy of $\phi^R_{a\bar{b}} = \left|\prod_k k\bar{k}.\, a\bar{b}\right|$

$$E^R_{a\bar{b}} = \left\langle \Phi^R_{a\bar{b}} \middle| H \middle| \Phi^R_{a\bar{b}} \right\rangle = E^R_{ab} + K_{ab}$$

gives access to the direct exchange integral,

$$< \Psi^1_N|H|\Psi^1_N > - < \Phi^R_{ab}|H|\,\Phi^R_{ab} > = < ab|ab > = 2K_{ab},$$

which is necessarily positive.

Since, according to the mirror theorem *a* and *b* are located on disjoint sets of atoms this integral is small. For the TS geometry the optimized SOMOs of the singlet and of the triplet are almost identical in restricted approaches. For the other geometries the *g* and *u* SOMOs of the triplet are close to the HOMO and LUMO of the CAS(2,2) of the singlet state. Beyond the direct exchange ferromagnetic correction $2K_{ab}$, two main contributions can be identified namely:

a) The mixing between Ψ^1_N and the "ionic" configuration away from TS geometry

$$\Psi^1_I = \left|\Pi_k k\bar{k}.(a\bar{a} + b\bar{b})\right| / \sqrt{2} = \left|\Pi_k k\bar{k}.(g\bar{g} + u\bar{u})\right| / \sqrt{2}\,,$$

where the two electrons are in the same SOMO and subject to a much larger repulsion. In WFT, the energy difference between the ionic and neutral configurations is called *U*,

$$U = \left\langle \Psi^1_I \middle| H \middle| \Psi^1_I \right\rangle - \left\langle \Psi^1_N \middle| H \middle| \Psi^1_N \right\rangle,$$

and they interact through a hopping integral $2t_{ab}$

$$\left\langle \Psi^1_N \middle| H \middle| \Psi^1_I \right\rangle = 2t_{ab},$$

in a 2x2 valence Configuration Interaction (CI) matrix

$$\begin{matrix} \Psi^1_N & \Psi^1_I \end{matrix}$$

$$\begin{pmatrix} K_{ab} & 2t_{ab} \\ 2t_{ab} & U + K_{ab} \end{pmatrix}$$

This interaction, solving the 2x2 CI matrix, results in an energy stabilization of the singlet, called "kinetic exchange"

$$\Delta KE = \frac{U - (U^2 + 16t_{ab}^2)^{1/2}}{2}$$

Of course there is no kinetic exchange contribution on the TS geometry since t_{ab} is then zero.

A BS calculation of the determinant

$$\Phi^{fc}_{a'\overline{b'}} = \left|\Pi_k k\bar{k}.\, a'\,\overline{b'}\right|$$

relaxing the magnetic orbitals in the field of the frozen core (fc) gives access to the values of the *t* and *U* parameter[11,16] through the knowledge of its energy lowering and of $\langle S^2 \rangle$

$$U = \frac{2(E^R_{a\bar{b}} - E^{U,fc}_{a'\bar{b}'})}{(1 - \langle S^2 \rangle^{U,fc}_{a'\bar{b}'})} - 2K_{ab},$$

$$|t_{ab}| = \frac{(E^R_{a\bar{b}} - E^{U,fc}_{a'\bar{b}'})}{(1 - \langle S^2 \rangle^{U,fc}_{a'\bar{b}'})^{1/2}}.$$

However, extracting t and U through the relaxation of the magnetic MOs is no longer valid when they lead to a closed-shell solution, and one requires to use a more general approach. This may be done by using the two non-optimized lowest closed-shell determinants, $|\prod k\bar{k}.\, g\bar{g}|$ and $\left|\prod k\bar{k}.\, u\bar{u}\right|$,

$$4t = E(\left|\Pi_k k\bar{k}.(g\bar{g})\right|) - E(\left|\Pi_k k\bar{k}.(u\bar{u})\right|)$$

$$U = E(\left|\Pi_k k\bar{k}.(g\bar{g})\right|) + E(\left|\Pi_k k\bar{k}.(u\bar{u})\right|) - E(\left|\Pi_k k\bar{k}.(gu)\right| + K_{ab}.$$

This alternative strategy results in a set of parameters consistent with those obtained by the orbital relaxation.[69]

b) The spin polarization of the core electrons by the exchange field of the unpaired electrons acting on the neutral component of the wave function is partly treated by relaxing

the core MOs in the differential exchange field of the unpaired electrons in the BS-DFT treatment, minimizing the energy of

$$\Phi_{Ua\bar{b}} = \left|\Pi_k k' \, \overline{k''}. a\bar{b}\right|$$

of energy $E_{a\bar{b}}$.

This function incorporates the effect of the singly-excited determinants

$$\Phi_{\bar{h}\to\bar{p},a\bar{b}} = \left|\Pi_{k\neq h} k\bar{k} \; h\bar{p} \; a\bar{b}\right|$$

and

$$\Phi_{h\to p,a\bar{b}} = \left|\Pi_{k\neq h} k\bar{k} \; p\bar{h} \; a\bar{b}\right|$$

but is not an S^2 eigenfunction. To satisfy this property one must include the spin-flip determinants

$$\Phi^{SF}_{\bar{h}\to\bar{p}} = \left|\Pi_{k\neq h} k\bar{k} \; \bar{h}\bar{p} \; ab\right|$$

$$\Phi^{SF}_{\bar{h}\to p} = \left|\Pi_{k\neq h} k\bar{k} \; hp \; \bar{a}\bar{b}\right|$$

which are doubly excited. Their effect may be called a spin-correlation effect between the unpaired electrons and the core electrons. It is proportional to that of the singly excited determinants, and it is possible to evaluate the energy brought by the spin-polarization and spin-correlation as

$$^1E_{SP} \cong 3(E_{U,a\bar{b}} - E_{a\bar{b}}).$$

This effect stabilizes the neutral component of the wave function. One may consider that one shifts the energy of the neutral component of the wave function by $^1E^{(2)}_{SP}$, and increases the effective value of *U* to *U'*

$$U' = U - {}^1E_{SP}.$$

The final energy of the singlet state is given by defining a

$$E_S = E^R_{ab} + 2K_{ab} + \frac{1}{2}\left(U' - (U'^2 + 16t^2_{ab})^{1/2}\right) + {}^1E_{SP}.$$

This procedure represents an extension of our previously proposed spin-decontaminated technique, exploiting BS solutions, to situations where spin-symmetry breaking does not occur between the HOMO and the LUMO to produce non-orthogonal SOMOs *a'* and *b'*. The method:

-starts from a restricted description of the lowest triplet state, which defines a pair of active MOs,

-constructs a 2x2 CI matrix between a neutral and an ionic configuration from mean values of closed-shell determinants,

-dresses this matrix under the spin-polarization effects obtained from constrained BS calculations,

-the final energy being the eigenvalue of the dressed CI matrix,

$$\begin{pmatrix} E_{a\bar{b}} + K_{ab} + {}^1E_{SP} & 2\,t_{ab} \\ 2\,t_{ab} & U + K_{ab} \end{pmatrix}$$

Notice that diagonalizing the dressed CI matrix by the spin polarization effects improves the weighting of the neutral component. We propose to call this procedure "DFT-dressed CI" (DFT-dCI).

C) Results

The overall results regarding the barriers are reported in Table 5 for the five members of the series, using different methods and different exchange correlation potentials. They should be compared with our best WFT estimates from large CASSCF + PT2 calculations.

The impact of the exchange correlation potential is crucial. According to Jacquemin *et. al* [70], BHHLYP and M06-2X deliver reasonably balanced description of the single and double bond lengths. If one simply relies on the energy difference between the CS single determinant for the bond-alternating geometry and the BS determinant for the "transition state", BHHLYP[24,25,71] functional increases the defect of B3LYP since the bond alternation is destroyed in all systems, including C_4H_4. M06-2X[72] functional restores barriers, with reasonable values of their heights at this crude level of description. On the basis of this study, M06-2X functional

may be considered as the best functional for the evaluation of the barrier heights in such systems.

The MRSF-TDDFT single point calculations using the CS and BS structures indicate barriers for all five species. This is in qualitative agreement with the CASPT2-IPEA-0.25 reference results. For the smallest C_4H_4 system, the error is as small as 0.8 kcal/mol. For the larger systems, MRSF-TDDFT tend to overestimate the barriers by about 5 kcal/mol. Other than the typical ~3 kcal/mol error in energy calculations (see above for the ST gap estimation), another possible factor is that the "active space" with two electrons in two orbitals of the MRSF-TDDFT formalism is relatively smaller for those large systems. All the π orbitals and electrons are not treated on the same footing, and this is especially so when the π space becomes larger. When the spin polarization within the π space is large, it is necessary to include the whole space in the zeroth-order description of the system, so that the cooperative spin polarization is treated in a self-consistent manner. The spin polarization is more significant at the TS structures. Therefore, the inability of treating spin polarization through one-electron spin-flipping from doubly occupied orbitals to virtual orbitals becomes more pronounced, resulting in an overestimated energy. For comparison, the spin polarization is less significant at the CS structure and therefore, this inability does not overestimate the energy as much. Consequently, the barrier is overestimated.

The electronic states of the MRSF-TDDFT calculations are consistent with expectation. At the CS geometries, the states are dominated by the $\left|\Pi_k k\overline{k}.\, g\overline{g}\right|$ closed-shell configurations, with the 0.98 amplitude for all five species. At the BS geometries, the states are dominated by the Ψ_N^1 open-shell configuration, with the amplitudes ranging from 0.97 to 0.98.

The DFT-dCI technique systematically improves the results with respect to the crude DFT values, stabilizing more the bond-alternating geometry than the TS, but does not provide sufficient barriers for B3LYP[24–27], nor for BHHLYP[24,25,71]. M06-2X[72] overestimates the barriers at the crude DFT level but DFT-dCI now diminishes them to a good agreement with the best WFT values. The DFT-dCI always works in the right direction. For intermediate structures connecting the diradical TS and closed shell minima, the mixed character of the wave function is frequently problematic.[73] This problem has been considered in the carbo-cyclobutadiene

$C_{12}H_4$. The DFT/MO6-2X-dCI presents satisfactory behavior as shown in Figure 4, the potential energy curve being in qualitative agreement with the Full π CASPT2 and NEVPT2 results.

Our DFT-dCI procedure enables us to identify the origin of the divergent values for different functionals. Table 6 summarizes the values of the t and U parameters which govern the neutral/ionic mixture and the kinetic exchange amplitude. The question of the dependence to the density functional approximation used, and especially the amount of exact exchange, has been intensively investigated in the context of magnetic couplings. The answer directly relies on the physics of the t and U parameters.[74–88] The hopping integral is weakly sensitive to the functional, while the effective bi-electronic repulsion U, although nearly identical in B3LYP and BHHLYP, is dramatically reduced by the M06-2X potential. This reduction increases the amplitude of the kinetic exchange, acting on the bond-alternating region, and increases the barrier. We think that the decomposition and consistent combination of the three contributions: direct exchange, kinetic exchange and spin-polarization, are both numerically effective and physically enlightening.

V) Conclusion

The problem of the evaluation of the barrier height in C_{4n} rings appears to be difficult. DFT/B3LYP approaches relying on energy minimizations of the CS determinant for the equilibrium geometry and of the BS open-shell determinant for the transition state underestimate or even suppress the barrier. The reasons of this unbalance have been analyzed and discussed, the TS is subject to a strong spin-polarization, the counterpart of which (a spin-correlation effect) is not considered in the CS treatment. Moreover, the CS function imposes equal weights to the neutral and ionic components of the outer-valence wave function.

The use of a minimal active space with 2 active electrons in either the HOMO and LUMO or in the two SOMOs seems in principle to solve this unbalance, but numerical explorations show that the so-calculated barriers are far too large, and that the subsequent second-order perturbation reverses the energetic order. This dramatic impact of the post-CAS energy is due to the large spin-polarization correction. Going to a full valence π CASSF treatment provides more reasonable values of the barrier, but it is necessary to perform an additional second-

order correction. In CASPT2 treatments, even with this large CAS, the IPEA shift is required to restore a barrier.

We have finally exploited the MRSF-TDDFT method and formulated an extension of the recently proposed spin-decontaminated DFT method[16] for the evaluation of the singlet-state energy via a consistent treatment of kinetic and spin-polarization effects. The current proposition can be extended to situations where the singlet state is no longer subject to Symmetry Breaking. Of low computational cost, it may be applied to large systems. Indeed, the here-addressed problem is not limited to the rather exotic problem of the isomerization barrier of C_{4n} rings. It concerns many isomerization problems between equilibrium geometries of essentially closed shell character, passing through a diradical transition state. Many isomerizations proceeding through the rotations around double bonds are of this type, but other reactions involve charge transfer transition state[73,89,90]. Cyclization reactions should also be considered.

In some sense the here-addressed question is linked to a more general problem, namely the dual vision of the molecular electronic population, either as composed of local on-bond electron pairs, or as of on delocalized energy-governed MOs. In the case of C_{4n} rings, at the transition-state geometry the on-bond localization[91,92] leads to two degenerate solutions, none of them being a satisfactory starting point for the building of the wave function. It is noteworthy that the symmetry-breaking taking place around this geometry calls the attention on a third representation of the electronic assembly as governed by effective spin antiferromagnetic interactions[93]. This multiplicity of viewpoints and entrance doors is not a defect but a richness of Quantum Chemistry.

Acknowledgments: G.D. benefits of research funding from the European Union's Horizon 2020 research and program under the Marie Skłodowska-Curie grant agreement No 899546. Mésocentre of Aix-Marseille Université is acknowledged for allocated HPC resources. T.Z. thanks York University for the start-up grant (481333) and the Natural Sciences and Engineering Research Council (NSERC) of Canada for funding (RGPIN-2016-06276), and thanks Compute Canada for computational resources.

Table 1: Calculated B3LYP/6-311G** CC bond lengths (Å) at equilibrium geometries for closed-shell and open-shell (broken-symmetry) solutions. Mean bond lengths are given, with standard deviations in parenthesis when required.

Systems	Closed shell geometry		Broken symmetry geometry*
	Short CC-bond (Å)	Long CC-bond (Å)	CC-bond (Å)
C_4H_4	1.332	1.579	1.444
$C_{12}H_4$**	1.211 (*a*) 1.261 (*a'*)	1.429 (*b*) 1.331 (*b'*)	1.234 1.380
$C_{13}H_{10}$	1.352 (0.001)	1.455 (0.001)	1.401 (0.000)
$C_{16}H_{16}$	1.360	1.449	1.403
$C_{19}H_{14}$	1.358 (0.003)	1.447 (0.003)	1.401 (0.003)

* All species are transition states, except for $C_{12}H_4$ and $C_{16}H_{16}$, which are true minima.

** The two lines refer to butyne and butatriene edges respectively (see labels in Figure 1)

Table 2. DFT/B3LYP calculations: $<S^2>$ and imaginary frequency (*i*) of the BS solution, barrier and corrected ZPE barrier between the two equivalent bond-alternating forms. For $C_{12}H_4$, the BS solution is a real minimum while the $C_{16}H_{16}$ BS is a local minimum.

			ΔE (kcal/mol)	
system	$<S^2>$	*i* (cm^{-1})	Barrier	ZPE
C_4H_4	1.05	405	2.2	-0.7
$C_{12}H_4$	1.12	-	(-2.9)	-5.0
$C_{13}H_{10}$	1.12	250	0.5	-2.4
$C_{16}H_{16}$	1.20	-	(-0.9)	-3.5
$C_{19}H_{14}$	1.18	365	1.0	-2.1

Table 3. Energy difference (kcal/mol) between open-shell and closed-shell minima obtained by means of single determinant (CS or BS) DFT/B3LYP and CASSCF+PT2 calculations with minimal CAS(2,2) active spaces. The main weights of the wave functions of the two states are also given.

	DFT B3LYP		CASSCF(2,2)	CASPT2 Ipea 0 a.u.	CASPT2 Ipea 0.25 a.u.	NEVPT2
C_4H_4	2.2	ΔE	12.1	-7.0	-1.3	0.7
		Weight (CS geo)	0.96 |20> 0.04 |02>			
		Weight (BS geo)	0.50 |20> 0.50 |02>			
$C_{12}H_4$	-2.7	ΔE	24.7	-17.6	-4.1	-20.6
		Weight (CS geo)	0.99 |20> 0.01 |02>			
		Weight (BS geo)	0.50 |20> 0.50 |02>			
$C_{13}H_{10}$	0.5	ΔE	25.2	-10.9	1.2	-10.9
		Weight (CS geo)	0.99 |20> 0.01 |02>			
		Weight (BS geo)	0.51 |20> 0.49 |02>			
$C_{16}H_{16}$	-0.9	ΔE	25.7	(11.3)	(11.5)	(4.8)
		Weight (CS geo)	0.997 |20> 0.003 |02>			
		Weight (BS geo)	0.98 |20> 0.02 |02>			
$C_{19}H_{14}$	1.0	ΔE	40.7	X	X	-8.1
		Weight (CS geo)	0.97 |20> 0.03 |02>			
		Weight (BS geo)	0.50 |20> 0.50 |02>			

Table 4. . Energy difference (kcal/mol) between open-shell and closed-shell minima obtained by means of CASSCF+PT2 calculations with full π active spaces. The main weights of the wave functions of the two states are also given, expressed on the HOMO/LUMO or SOMOs.

	CAS Full π				
		CASSCF	CASPT2 Ipea 0 a.u.	CASPT2 Ipea 0.25 a.u.	SC-NEVPT2
C_4H_4	ΔE	6.1	3.3	6.4	8.4
	Weight (CS geo)	0.88 |20> 0.04 |02>			
	Weight (BS geo)	0.46 |20> 0.46 |02>			
$C_{12}H_4$	ΔE	6.1	-1.9	2.6	2.3
	Weight (CS geo)	0.75 |20> 0.03 |02>			
	Weight (BS geo)	0.36 |20> 0.36 |02>			
$C_{13}H_{10}$	ΔE	9.4	0.0	5.1	4.4
	Weight (CS geo)	0.74 |20> 0.02 |02>			
	Weight (BS geo)	0.35 |20> 0.34 |02>			
$C_{16}H_{16}$	ΔE	10.3	-1.5	4.4	4.6
	Weight (CS geo)	0. |20> 0.01 |02>			
	Weight (BS geo)	0.27 |20> 0.27 |02>			
$C_{19}H_{14}$	ΔE	11.8	-0.2	6.0	
	Weight (CS geo)	0.66 |20> 0.01 |02>			
	Weight (BS geo)	0.51 |11> 0.04 |20> 0.04 |02>			

Table 5. Energy difference (kcal/mol) between open-shell (OS) and closed-shell (CS) minima obtained by means of single determinant (CS or OS) DFT or DFT-dressed CI (DFT-dCI) using different functionals and MRSF-TDDFT/BHHLYP.

	C_4H_4	$C_{12}H_4$	$C_{13}H_{10}$	$C_{16}H_{16}$	$C_{19}H_{14}$
CASPT2-IPEA 0.25 (table 4)	6.4	2.6	5.1	4.4	6.0
DFT/B3LYP	2.2	-2.7	0.5	-0.9	1.1
DFT-dCI B3LYP	5.6	-0.9	1.2	0.0	1.0
DFT/M06-2X	6.7	2.5	6.3	5.5	7.6
DFT-dCI M06-2X	8.6	1.1	4.5	2.9	4.3
DFT / BHHLYP	-5.3	-9.7	-5.9	-10.1	93.4*
DFT-dCI / BHHLYP	1.5	-4.3	-2.3	-4.0	-3.7
MRSF-TDDFT/BHHLYP	5.6	7.2	9.7	9.4	11.0

* $\langle S^2 \rangle = 1.57$

Table 6. Hopping integral t and on-site repulsion U (in a.u.) from various functionals in the case of carbomerized cyclobutadiene.

	B3LYP	M06-2X	BHHLYP
t	-0.0171831	-0.020175	-0.020851
U	0.0230019	0.0158654	0.0243505

Figure 1. Structures of the five C_{4n} rings: cyclobutadiene C_4H_4, carbo-cyclobutadiene $C_{12}H_4$, centro-saturated phenalene $C_{13}H_{10}$, crown-shaped $C_{16}H_{16}$ and internally saturated C_{16} ring

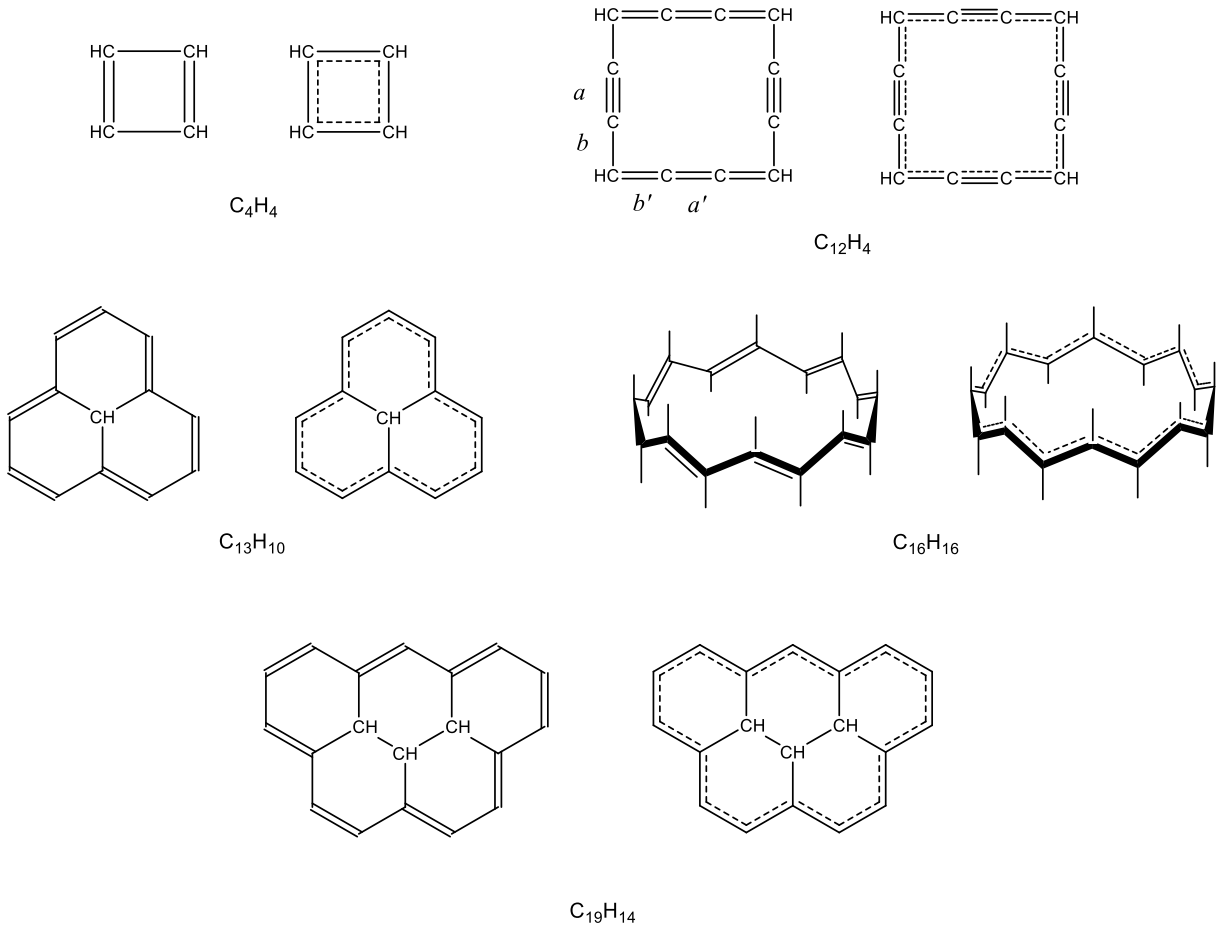

Figure 2. HOMO/LUMO and SOMOs of the five C_{4n} rings obtained at the full π CASSCF level.

	MOs CS geometry		MOs BS geometry	
C_4H_4	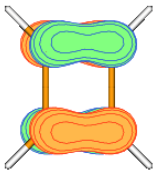	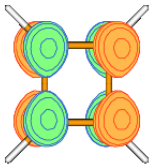	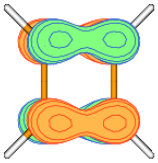	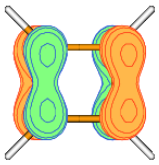
$C_{12}H_4$	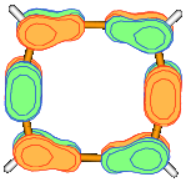	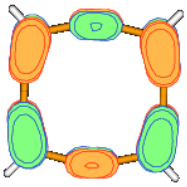	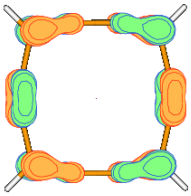	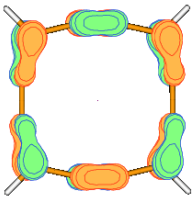
$C_{13}H_{10}$	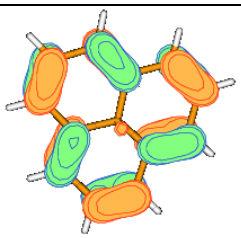	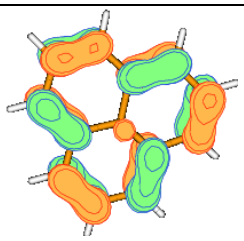	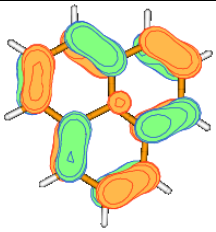	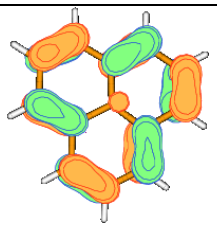
$C_{16}H_{16}$	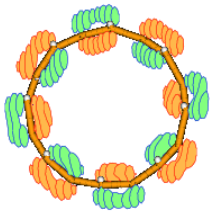	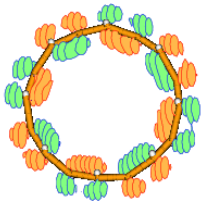	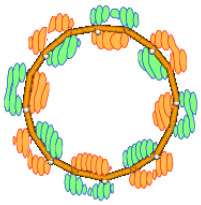	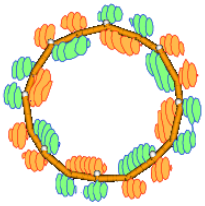
$C_{19}H_{14}$	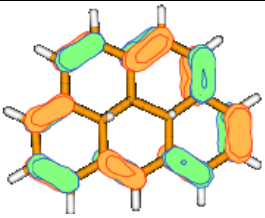	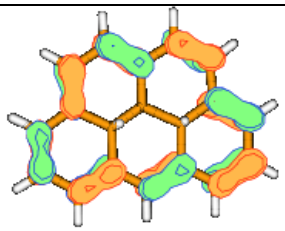	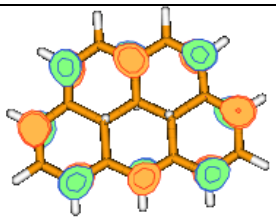	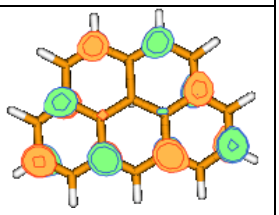

Figure 3. Evolution of the DFT/B3LYP energy as a function of the geometry of the carbomerized cyclobutadiene $C_{12}H_4$ for the BS (ms=0) and the closed shell singlet. LST stands for linear synchronous transit.

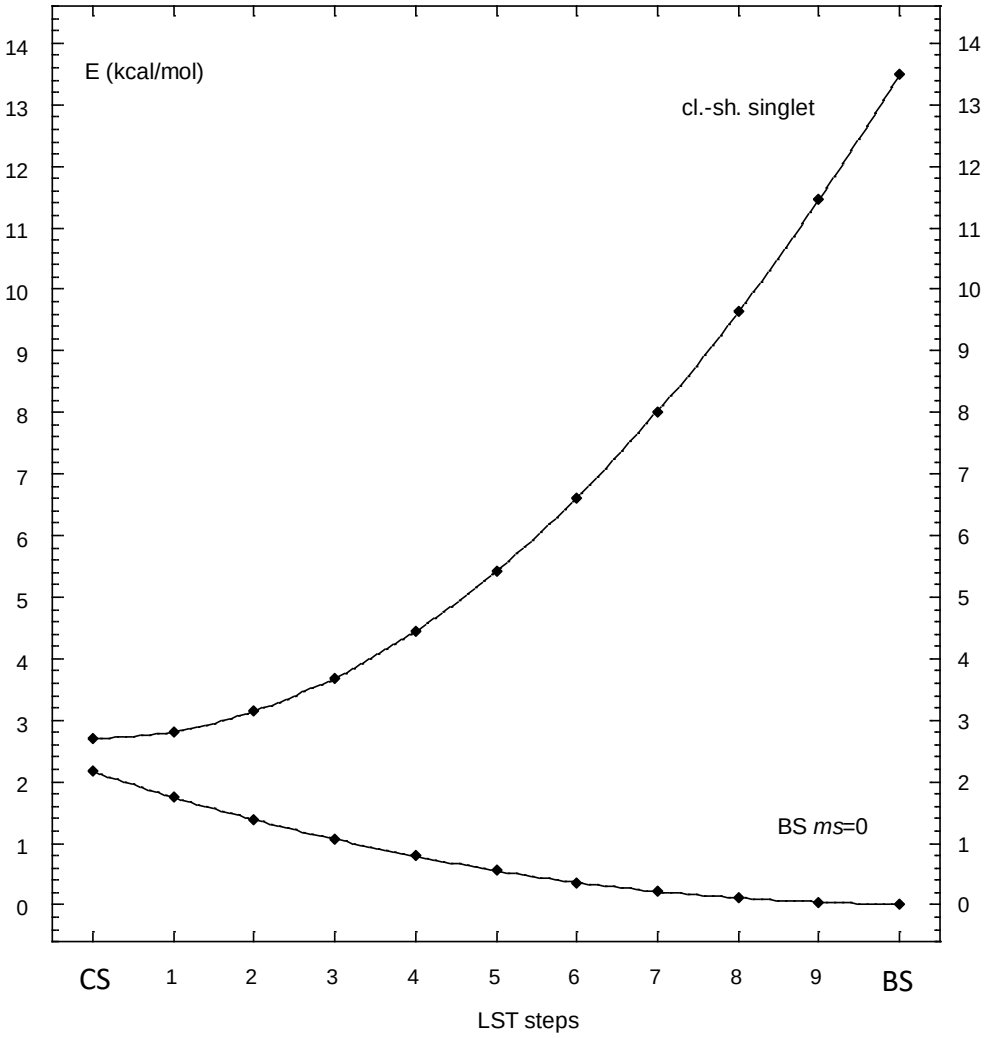

Figure 4. Evolution of the full π CAS(12,12) based energies as a function of the geometry of the carbo-cyclobutadiene $C_{12}H_4$.The zero of energy has been taken at the BS geometry. LST stands for linear synchronous transit.

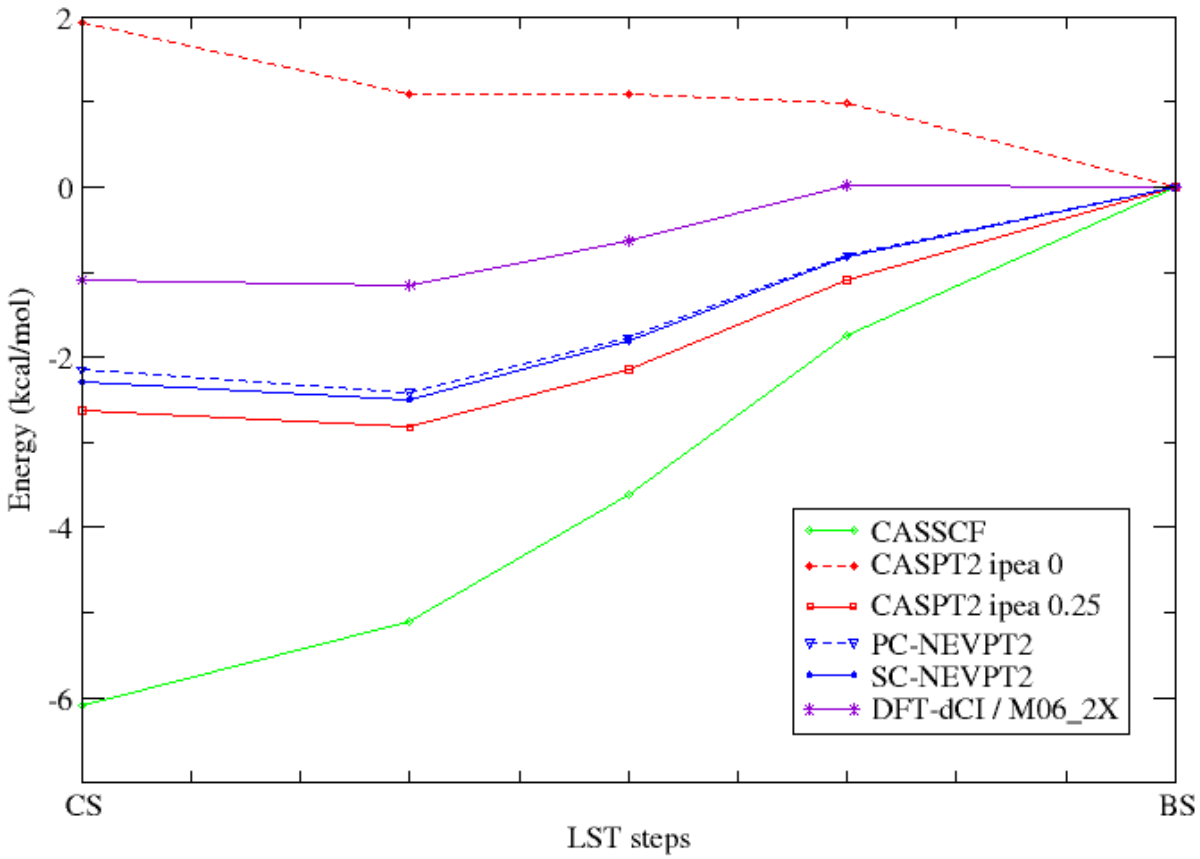

[1] H.A. Jahn and E. Teller, Proc. R. Soc. Lond. A **161**, 220 (1937).
[2] R.G. Pearson, Journal of Molecular Structure: THEOCHEM **103**, 25 (1983).
[3] A.F. Voter and W.A. Goddard, J. Am. Chem. Soc. **108**, 2830 (1986).
[4] K. Nakamura, Y. Osamura, and S. Iwata, Chemical Physics **136**, 67 (1989).
[5] G. Berthier, J. Chim. Phys. **51**, 363 (1954).
[6] J.A. Pople and R.K. Nesbet, J. Chem. Phys. **22**, 571 (1954).
[7] L. Noodleman, J. Chem. Phys. **74**, 5737 (1981).
[8] K. Yamaguchi, H. Fukui, and T. Fueno, Chem. Lett. **15**, 625 (1986).
[9] K. Yamaguchi, Y. Takahara, T. Fueno, and K.N. Houk, Theoret. Chim. Acta **73**, 337 (1988).
[10] S. Yamanaka, M. Okumura, M. Nakano, and K. Yamaguchi, J MOL STRUC-THEOCHEM **310**, 205 (1994).
[11] R. Caballol, O. Castell, F. Illas, I. de P. R. Moreira, and J.P. Malrieu, J. Phys. Chem. A **101**, 7860 (1997).
[12] T. Tsuchimochi and G.E. Scuseria, J. Chem. Phys. **134**, 064101 (2011).
[13] C.A. Jiménez-Hoyos, T.M. Henderson, T. Tsuchimochi, and G.E. Scuseria, J. Chem. Phys. **136**, 164109 (2012).
[14] N. Ferré, N. Guihéry, and J.-P. Malrieu, Phys. Chem. Chem. Phys. **17**, 14375 (2015).
[15] G. David, N. Ferré, G. Trinquier, and J.-P. Malrieu, J. Chem. Phys. **153**, 054120 (2020).
[16] G. David, G. Trinquier, and J.-P. Malrieu, J. Chem. Phys. **153**, 194107 (2020).
[17] M. Filatov and S. Shaik, Chem. Phys. Lett. **304**, 429 (1999).
[18] H.R. Zhekova, M. Seth, and T. Ziegler, J. Chem. Phys. **135**, 184105 (2011).
[19] B. Kaduk, T. Kowalczyk, and T. Van Voorhis, Chem. Rev. **112**, 321 (2012).
[20] Y. Shao, M. Head-Gordon, and A.I. Krylov, J. Chem. Phys. **118**, 4807 (2003).
[21] S.J. Stoneburner, D.G. Truhlar, and L. Gagliardi, J. Chem. Phys. **148**, 064108 (2018).
[22] S. Lee, M. Filatov, S. Lee, and C.H. Choi, J. Chem. Phys. **149**, 104101 (2018).
[23] B.O. Roos, P.R. Taylor, and P.E.M. Siegbahn, Chem. Phys. **48**, 157 (1980).
[24] A.D. Becke, J. Chem. Phys. **98**, 5648 (1993).
[25] C. Lee, W. Yang, and R.G. Parr, Phys. Rev. B **37**, 785 (1988).
[26] S.H. Vosko, L. Wilk, and M. Nusair, Can. J. Phys. **58**, 1200 (1980).
[27] P.J. Stephens, F.J. Devlin, C.F. Chabalowski, and M.J. Frisch, J. Phys. Chem. **98**, 11623 (1994).
[28] N. Ben Amor, C. Noûs, G. Trinquier, and J.-P. Malrieu, J. Chem. Phys. **153**, 044118 (2020).
[29] A.A. Ovchinnikov, Theoret. Chim. Acta **47**, 297 (1978).
[30] E.H. Lieb, Phys. Rev. Lett. **62**, 1201 (1989).
[31] J.-P. Malrieu, N. Ferré, and N. Guihéry, in *Applications of Topological Methods in Molecular Chemistry*, edited by R. Chauvin, C. Lepetit, B. Silvi, and E. Alikhani (Springer International Publishing, Cham, 2016), pp. 361–395.
[32] H.C. Longuet-Higgins, J. Chem. Phys. **18**, 265 (1950).
[33] K. Andersson, P.-Å. Malmqvist, B.O. Roos, A.J. Sadlej, and K. Wolinski, J. Phys. Chem. **94**, 5483 (1990).
[34] G. Ghigo, B.O. Roos, and P.-Å. Malmqvist, Chem. Phys. Lett. **396**, 142 (2004).
[35] C. Angeli, R. Cimiraglia, S. Evangelisti, T. Leininger, and J.-P. Malrieu, J. Chem. Phys. **114**, 10252 (2001).
[36] C. Angeli, R. Cimiraglia, and J.-P. Malrieu, J. Chem. Phys. **117**, 9138 (2002).
[37] M. Kepenekian, V. Robert, and B. Le Guennic, J. Chem. Phys. **131**, 114702 (2009).
[38] F. Ruipérez, F. Aquilante, J.M. Ugalde, and I. Infante, J. Chem. Theory Comput. **7**, 1640 (2011).
[39] A. Kerridge, Phys. Chem. Chem. Phys. **15**, 2197 (2013).

[40] M. Radoń, P. Rejmak, M. Fitta, M. Bałanda, and J. Szklarzewicz, Phys. Chem. Chem. Phys. **17**, 14890 (2015).
[41] S. Vela, M. Fumanal, J. Ribas-Ariño, and V. Robert, J Comput Chem **37**, 947 (2016).
[42] S. Vancoillie, P.Å. Malmqvist, and V. Veryazov, J. Chem. Theory Comput. **12**, 1647 (2016).
[43] J.P. Zobel, J.J. Nogueira, and L. Gonzalez, Chem. Sci. **8**, 1482 (2017).
[44] C. Wiebeler, V. Borin, A.V. Sanchez de Araújo, I. Schapiro, and A.C. Borin, Photochemistry and Photobiology **93**, 888 (2017).
[45] N. Ben Amor, A. Soupart, and M.-C. Heitz, Journal of Molecular Modeling **23**, (2017).
[46] R. Sarkar, P.-F. Loos, M. Boggio-Pasqua, and D. Jacquemin, J. Chem. Theory Comput. **18**, 2418 (2022).
[47] M. J. Frisch, G. W. Trucks, H. B. Schlegel, G. E. Scuseria, M. A. Robb, J. R. Cheeseman, G. Scalmani, V. Barone, G. A. Petersson, H. Nakatsuji, X. Li, M. Caricato, A. V. Marenich, J. Bloino, B. G. Janesko, R. Gomperts, B. Mennucci, H. P. Hr, *Gaussian 09* (Gaussian, Inc., Wallingford CT, 2013).
[48] G. Karlström, R. Lindh, P.-Å. Malmqvist, B.O. Roos, U. Ryde, V. Veryazov, P.-O. Widmark, M. Cossi, B. Schimmelpfennig, P. Neogrady, and L. Seijo, Comput. Mater. Sci. **28**, 222 (2003).
[49] V. Veryazov, P.-O. Widmark, L. Serrano-Andrés, R. Lindh, and B.O. Roos, Int. J. Quantum Chem. **100**, 626 (2004).
[50] F. Aquilante, L. De Vico, N. Ferré, G. Ghigo, P.Å. Malmqvist, P. Neogrády, T.B. Pedersen, M. Pitoňák, M. Reiher, B.O. Roos, L. Serrano-Andrés, M. Urban, V. Veryazov, and R. Lindh, J Comput Chem **31**, 224 (2010).
[51] G.M.J. Barca, C. Bertoni, L. Carrington, D. Datta, N. De Silva, J.E. Deustua, D.G. Fedorov, J.R. Gour, A.O. Gunina, E. Guidez, T. Harville, S. Irle, J. Ivanic, K. Kowalski, S.S. Leang, H. Li, W. Li, J.J. Lutz, I. Magoulas, J. Mato, V. Mironov, H. Nakata, B.Q. Pham, P. Piecuch, D. Poole, S.R. Pruitt, A.P. Rendell, L.B. Roskop, K. Ruedenberg, T. Sattasathuchana, M.W. Schmidt, J. Shen, L. Slipchenko, M. Sosonkina, V. Sundriyal, A. Tiwari, J.L. Galvez Vallejo, B. Westheimer, M. Włoch, P. Xu, F. Zahariev, and M.S. Gordon, J. Chem. Phys. **152**, 154102 (2020).
[52] F. Neese, F. Wennmohs, U. Becker, and C. Riplinger, J. Chem. Phys. **152**, 224108 (2020).
[53]It is worth noting that the Gaussian implementation of the B3LYP functional has been employed in this work, used through the keyword B3LYP/G in the Orca package.
[54] H.-L. Lee and W.-K. Li, Org. Biomol. Chem. **1**, 2748 (2003).
[55] C. Castro, Z. Chen, C.S. Wannere, H. Jiao, W.L. Karney, M. Mauksch, R. Puchta, N.J.R. van E. Hommes, and P. von R. Schleyer, J. Am. Chem. Soc. **127**, 2425 (2005).
[56] R.P. Pemberton, C.M. McShane, C. Castro, and W.L. Karney, J. Am. Chem. Soc. **128**, 16692 (2006).
[57] S. Taubert, D. Sundholm, and F. Pichierri, J. Org. Chem. **74**, 6495 (2009).
[58] C. Gellini and P.R. Salvi, Symmetry **2**, 1846 (2010).
[59] C.S. Michel, P.P. Lampkin, J.Z. Shezaf, J.F. Moll, C. Castro, and W.L. Karney, J. Am. Chem. Soc. **141**, 5286 (2019).
[60] J.K. Arbitman, C.S. Michel, C. Castro, and W.L. Karney, Org. Lett. **21**, 8587 (2019).
[61] I. Casademont-Reig, E. Ramos-Cordoba, M. Torrent-Sucarrat, and E. Matito, Molecules **25**, 711 (2020).
[62] A. Balková and R.J. Bartlett, J. Chem. Phys. **101**, 8972 (1994).
[63] N. Suaud, N. Ben Amor, N. Guihéry, and J.-P. Malrieu, Theor. Chem. Acc. **140**, 117 (2021).
[64] S. Lee, E.E. Kim, H. Nakata, S. Lee, and C.H. Choi, J. Chem. Phys. **150**, 184111 (2019).

[65] Y. Horbatenko, S. Sadiq, S. Lee, M. Filatov, and C.H. Choi, J. Chem. Theory Comput. **17**, 848 (2021).
[66] J.S. Sears, C.D. Sherrill, and A.I. Krylov, The Journal of Chemical Physics **118**, 9084 (2003).
[67] J.P. Malrieu, R. Caballol, C.J. Calzado, C. de Graaf, and N. Guihéry, Chem. Rev. **114**, 429 (2014).
[68] M. Huix-Rotllant, B. Natarajan, A. Ipatov, C. Muhavini Wawire, T. Deutsch, and M.E. Casida, Phys. Chem. Chem. Phys. **12**, 12811 (2010).
[69] C.J. Calzado, J. Cabrero, J.P. Malrieu, and R. Caballol, J. Chem. Phys. **116**, 2728 (2002).
[70] G. David, N. Guihéry, and N. Ferré, J. Chem. Theory Comput. **13**, 6253 (2017).
[71] D. Jacquemin and C. Adamo, J. Chem. Theory Comput. **7**, 369 (2011).
[72] A.D. Becke, Phys. Rev. A **38**, 3098 (1988).
[73] Y. Zhao and D.G. Truhlar, Theor. Chem. Acc. **120**, 215 (2008).
[74] S. Gozem, M. Huntress, I. Schapiro, R. Lindh, A.A. Granovsky, C. Angeli, and M. Olivucci, J. Chem. Theory Comput. **8**, 4069 (2012).
[75] R.L. Martin and F. Illas, Phys. Rev. Lett. **79**, 1539 (1997).
[76] F. Illas and R.L. Martin, J. Chem. Phys. **108**, 2519 (1998).
[77] C.J. Calzado, J. Cabrero, J.P. Malrieu, and R. Caballol, J. Chem. Phys. **116**, 3985 (2002).
[78] I. de P. R. Moreira, F. Illas, and R.L. Martin, Phys. Rev. B **65**, 155102 (2002).
[79] I. Ciofini, F. Illas, and C. Adamo, J. Chem. Phys. **120**, 3811 (2004).
[80] F. Illas, I. de P. R. Moreira, J.M. Bofill, and M. Filatov, Phys. Rev. B **70**, 132414 (2004).
[81] E. Ruiz, S. Alvarez, J. Cano, and V. Polo, J. Chem. Phys. **123**, 164110 (2005).
[82] F. Illas, I. de P.R. Moreira, J.M. Bofill, and M. Filatov, Theor Chem Acc **116**, 587 (2006).
[83] R. Valero, R. Costa, I. de P. R. Moreira, D.G. Truhlar, and F. Illas, J. Chem. Phys. **128**, 114103 (2008).
[84] S. Zein, M. Poor Kalhor, L.F. Chibotaru, and H. Chermette, J. Chem. Phys. **131**, 224316 (2009).
[85] J.J. Phillips and J.E. Peralta, J. Chem. Phys. **134**, 034108 (2011).
[86] J.J. Phillips, J.E. Peralta, and B.G. Janesko, J. Chem. Phys. **134**, 214101 (2011).
[87] E. Ruiz, J. Comput. Chem. **32**, 1998 (2011).
[88] J.J. Phillips and J.E. Peralta, J. Chem. Theory Comput. **8**, 3147 (2012).
[89] G. David, N. Guihéry, and N. Ferré, J. Chem. Theory Comput. **13**, 6253 (2017).
[90] X. Xu, S. Gozem, M. Olivucci, and D.G. Truhlar, J. Phys. Chem. Lett. **4**, 253 (2013).
[91] M. Huix-Rotllant, M. Filatov, S. Gozem, I. Schapiro, M. Olivucci, and N. Ferré, J. Chem. Theory Comput. **9**, 3917 (2013).
[92] C. Edmiston and K. Ruedenberg, Rev. Mod. Phys. **35**, 457 (1963).
[93] C. Edmiston and K. Ruedenberg, J. Chem. Phys. **43**, S97 (1965).
[94] D. Maynau, M. Said, and J.P. Malrieu, J. Am. Chem. Soc. **105**, 5244 (1983).

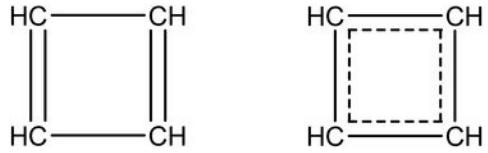

C_4H_4

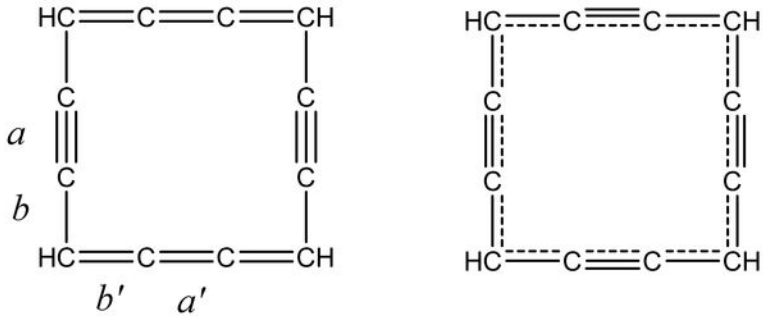

$C_{12}H_4$

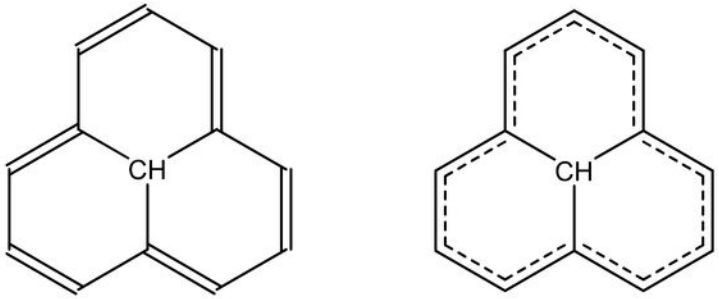

$C_{13}H_{10}$

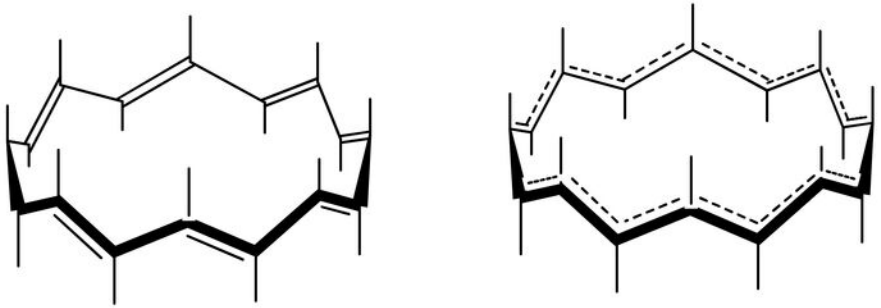

$C_{16}H_{16}$

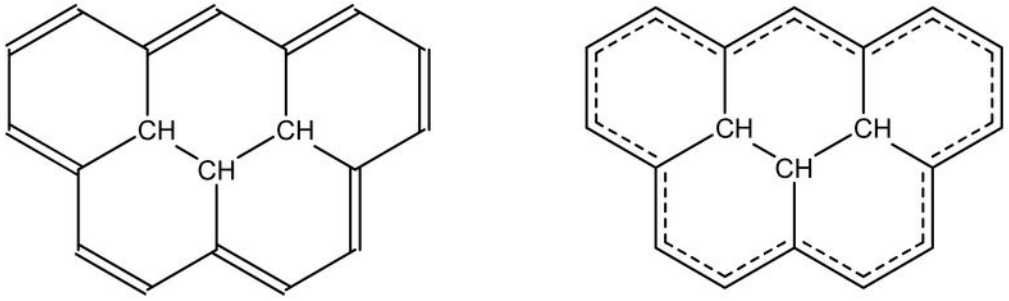

$C_{19}H_{14}$

	MOs CS geometry		MOs BS geometry	
C_4H_4	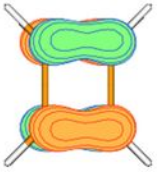	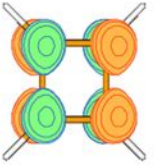	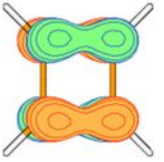	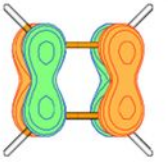
$C_{12}H_4$	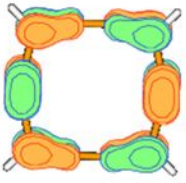	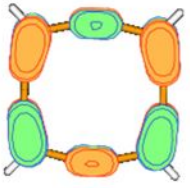	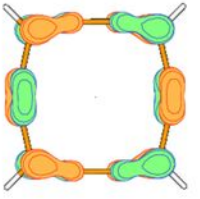	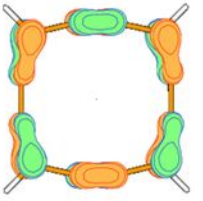
$C_{13}H_{10}$	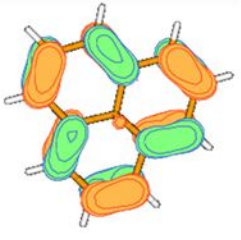	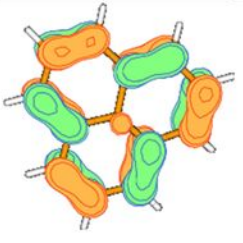	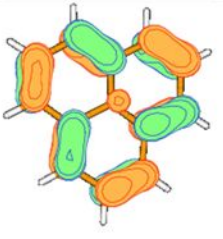	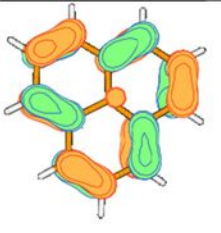
$C_{16}H_{16}$	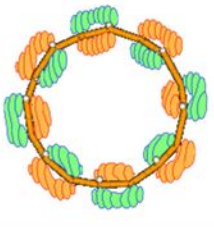		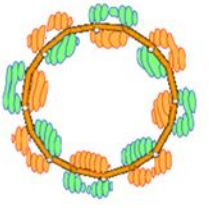	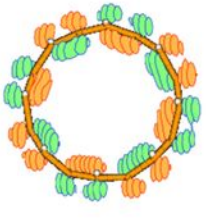
$C_{19}H_{14}$	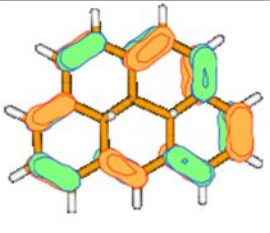	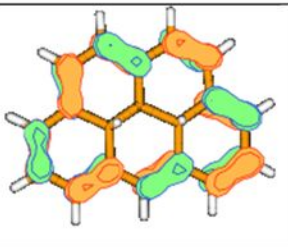	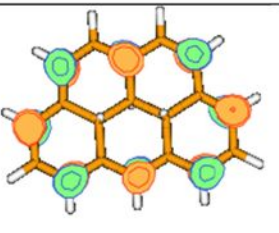	

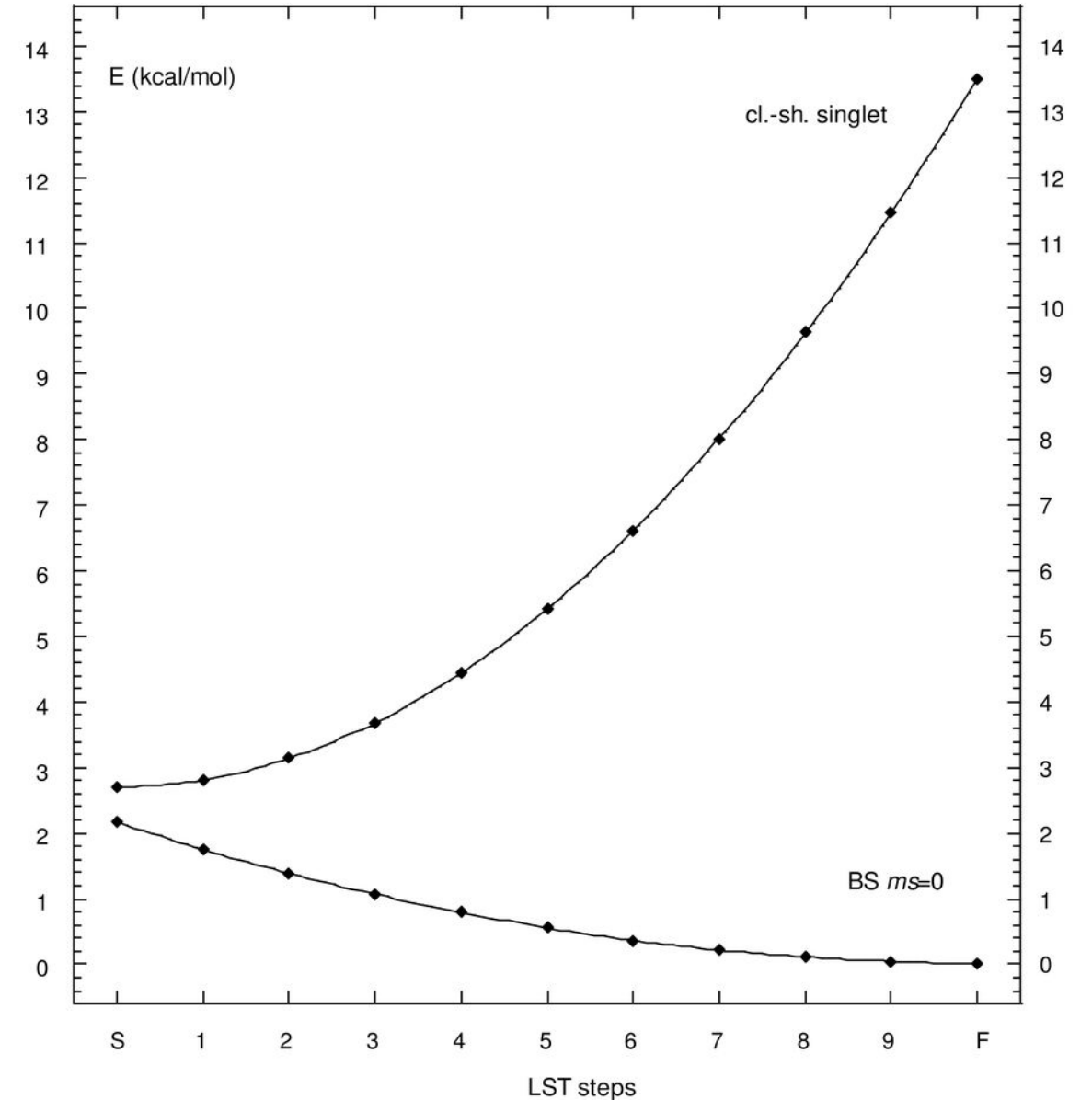
E (kcal/mol)
cl.-sh. singlet
BS ms=0
14
13
12
11
10
9
8
7
6
5
4
3
2
1
0
S
1
2
3
4
5
6
7
8
9
F
LST steps

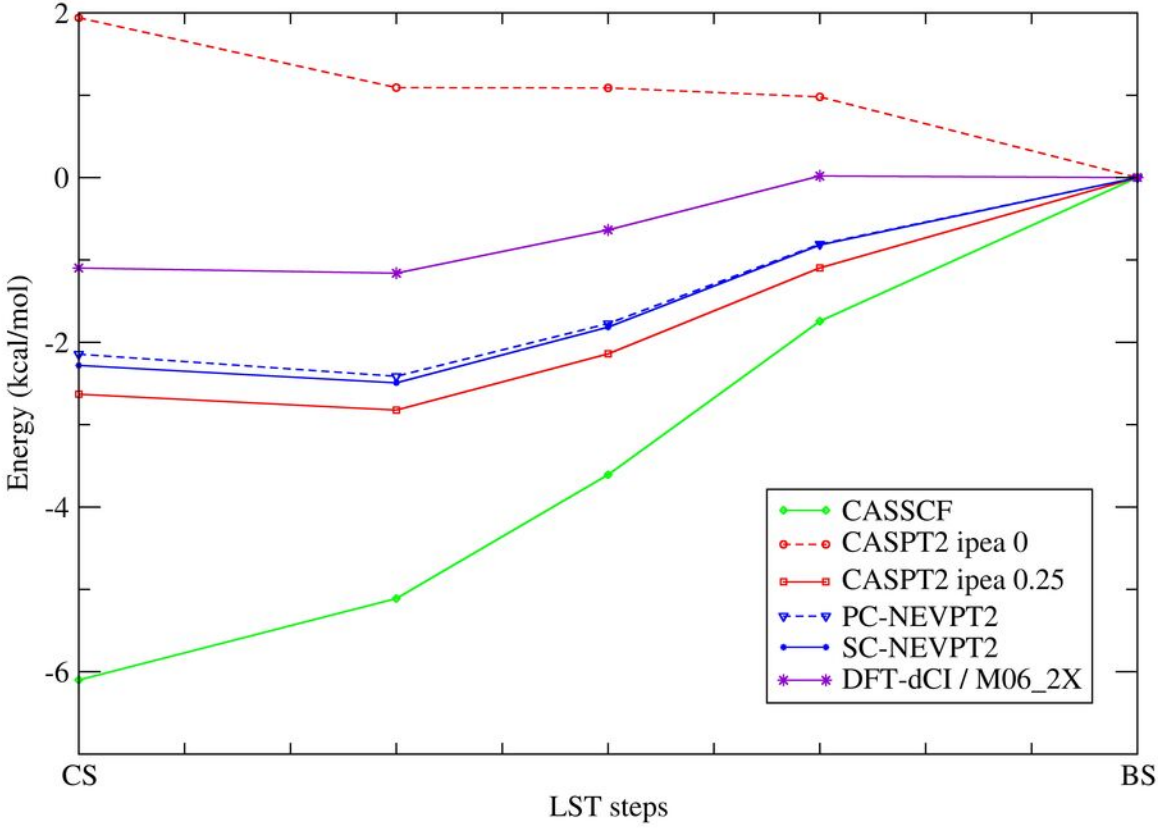
2
0
-2
-4
-6
Energy (kcal/mol)
CS
BS
LST steps
CASSCF
CASPT2 ipea 0
CASPT2 ipea 0.25
PC-NEVPT2
SC-NEVPT2
DFT-dCI / M06_2X